

—Original—

Investigation of spinal nerve ligation-mediated functional activation of the rat brain using manganese-enhanced MRI

Keun-Yeong JEONG¹⁾ and Ji-Hyuk KANG²⁾

¹⁾R&D division, Metimedi Pharmaceuticals, Suite 908, 263 Central-ro Yeonsu-gu, Incheon 22006, Republic of Korea

²⁾Department of Biomedical Laboratory Science, College of Health and Medical Science, Daejeon University, 62 Daehak-ro, Dong-gu, Daejeon 34520, Republic of Korea

Abstract: To provide clear information on the cerebral regions according to peripheral neuropathy, the functional activation was investigated using manganese-enhanced magnetic resonance imaging (MEMRI). L5-spinal nerve ligation (SNL) was applied to the rats to induce neuropathic pain. Mechanical allodynia and thermal hyperalgesia were measured to confirm neuropathic pain induction following before and after gabapentin (GBP) treatment. The cerebral regions were investigated using a 4.7T MRI system in the sham, SNL, and GBP-treated SNL rats. Neuropathic pain was severely induced by SNL on the postoperative day 14, excepting the sham group. While MEMRI indicated many activation regions in the brain of SNL rats before GBP treatment, the activities were chronologically attenuated after GBP treatment. The brain regions relating SNL-induced neuropathic pain were as follows: the posterior association area of the parietal region, superior colliculus, inferior colliculus, primary somatosensory area, cingulate cortex, and cingulum bundle. SNL induced- neuropathic pain is transmitted to the primary somatosensory area and parietal region through the cingulum bundle and limbic system. These findings would be helpful for the understanding of neuropathic pain-associated process and be an accurate target for a relief of neuropathic pain.

Key words: gabapentin, manganese-enhanced MRI, neuropathic pain, rat brain, spinal nerve ligation

Introduction

In neuropathic pain, the nerve fibers themselves may be damaged, dysfunctional, or injured [12]. Neuropathic pain characterized by an exaggerated response to non-noxious stimuli that is referred to as allodynia [15]. A study using an animal model for neuropathic pain has been conducted mainly through a behavioral test and a molecular biological analysis [16]. A novel approach was developed as the results of the research, but since

the central nervous system (CNS) regions, which are directly affected by the damage, have not been discovered, studies on them through multilateral approaches such as an imaging method are being conducted [2, 7].

The magnetic resonance imaging (MRI) techniques, based on blood oxygen level-dependent contrast, rely on changes in the brain hemodynamics during increased neural activity [19]. In addition, a manganese-based MRI technique (MEMRI) was recently described as being independent of hemodynamic changes [8]. MEMRI pro-

(Received 28 March 2017 / Accepted 13 July 2017 / Published online in J-STAGE 26 July 2017)

Address corresponding: J.-H. Kang, Department of Biomedical Laboratory Science, College of Health and Medical Science, Daejeon University, 62 Daehak-ro, Dong-gu, Daejeon 34520, Republic of Korea



This is an open-access article distributed under the terms of the Creative Commons Attribution Non-Commercial No Derivatives (by-nc-nd) License <<http://creativecommons.org/licenses/by-nc-nd/4.0/>>.

vides functional biological information and specific anatomical information in an animal model using manganese (Mn^{2+}) as a detectable contrast agent [11].

Since voltage-gated calcium (Ca^{2+}) channels are found in a wide range of tissues, it might be possible to use Mn^{2+} to assess Ca^{2+} influx by MRI. When Mn^{2+} reach the nerve endings, they are released into the synaptic cleft, where they can traverse the postsynaptic membrane through voltage-gated Ca^{2+} channels. Therefore, more excitable nervous tissue can result from more Mn^{2+} accumulation, leading to a strong signal intensity in the T1-weighted image following MEMRI.

Gabapentin (GBP) is a structural analogue of gamma-aminobutyric acid (GABA) that is thought to block the $\alpha 2\delta$ subunit of voltage-dependent Ca^{2+} channels in dorsal horn postsynaptic cells. To enhance GABAergic transmission, it has been hypothesized that GBP modulates voltage-gated Ca^{2+} channels, resulting in decreased glutamatergic neurotransmitter release [25]. Therefore, GBP was originally developed for the treatment of epileptic seizure, but it is currently also used to relieve neuropathic pain [17].

The purpose of this work was to provide clear information on the regions activated during peripheral neuropathy in the rat brain. To achieve this, activated regions of the brain were analyzed using the MEMRI in the neuropathic pain-induced rats.

Materials and Methods

Animals

All experiments were performed under the institutional guidelines established by the Institutional Animal Care and Use Committee at Gachon University (IACUC-2014-0177). Total 35 Sprague-Dawley (SD) rats were obtained from Samtako Co. (Osan, South Korea). And, 6-week of age male SD rats were used in the present study. All animals were maintained in a 12-h light/dark cycle (light on, 08:00) at 22–25°C with free access to food and water.

Spinal nerve ligation model

The animals were placed in a small acrylic cage that was coupled with an anesthesia machine that allowed them to breathe freely under gaseous anesthesia (2% isoflurane, Spartanburg, SC, USA). And then, peripheral nerve injury was induced via L5 spinal nerve ligation (SNL) as previously described [5]. The para-spinal

muscles were spread using surgical scissors and removed the L5-S1 spinal processes. After the steps, the L5 nerve was isolated and ligated tightly with 5–0 silk thread. The surgical operation was performed only up to step for removing L5-S1 spinal processes to establish sham group.

Mechanical allodynia test

The paw withdrawal threshold for mechanical stimuli was used as an indicator of intense degree of neuropathic pain. Mechanical sensitivity was measured by a von Frey filament (Stoelting, IL, USA) using the up-and-down paradigm [1, 3].

Thermal hyperalgesia test

To assess hindpaw thermal pain sensitivity, a modified Hargreaves' test was conducted according to the procedures of previous studies [18]. Cold hyperalgesia was measured using the acetone drop test following an already established method by Dècosterd and Woolf [6].

Cannula implantation for administration

The animals were placed in a small acrylic cage and allowed to breathe freely under gaseous anesthesia. After full anesthesia, the animal fur was shaved with an electric clipper from the posterior region of the neck to the occiput, and the skin was swabbed with iodine. The midline of the posterior region of the neck skin was vertically sectioned into 1-cm part. Then, an incision was made directly into the midline of the triple layers of muscle, and the muscles were spread with surgical scissors. After these steps, the cisterna magna was visible between the muscles. Then, a 30-mm PE10 polyethylene tube (BD bioscience, Franklin Lakes, NJ, USA) was carefully inserted into the cerebral ventricle through the cisterna magna. A 27.5-gauge needle and 5-mm PE20 polyethylene tube (BD bioscience, Franklin Lakes, NJ, USA) were used as an entrance cover for the PE10 tube.

GBP treatment

For the measurement of behavior response and MEMRI scanning, 17.5 $\mu M/50 \mu l$ of GBP was intracerebroventricularly administered to the neuropathic pain-induced rat 30 min before each experiment using a Hamilton syringe (Hamilton Co., Reno, NV, USA).

Contrast agent

$MnCl_2 \cdot 4H_2O$ (Sigma, St. Louis, MO, USA) was used

as a contrast agent for MEMRI. The 20 mM of MnCl_2 was dissolved in pH-buffered physiological saline and was kept at up to 4°C. The contrast agent was manually injected 24 h before MEMRI via the implanted cannula using a 27-gauge needle under gaseous anesthesia (2% isoflurane) as previously described [13].

MEMRI sequences

The anatomical images of the rat brain were acquired 24 h after the contrast agent administration as described in a previous study [13]. Isoflurane was used to maintain the anesthetization (induction 4% and maintenance 2%) for MEMRI. The rats were placed on an experimental cradle, and warm water went through the pipe underneath the cradle to prevent temperature decline. Regarding physiological monitoring, the stability of breathing was observed by respiration sensor. MRI were performed using a 4.7T MRI system (Bruker, BioSpec 47/40, Karlsruhe, Germany). A rat brain surface coil as RF receiver and the 72 mm volume coil as RF transmitter were used (Bruker, Biospin, Rheinstetten, Germany). For analyzing the contrast agent distribution, a set of continuous two dimensional (2D) multi-slice T_1 -weighted images using spin-echo pulse sequence were acquired. T_1 -weighted images were performed with the following imaging parameters; repetition time=400 ms, echo time=10.5 ms, number of averages=8, number of slices=24, slice thickness=0.5 mm, flip angle=90°, field of view=width 40 × length 30 mm², matrix size=256 × 256, leading to a voxel size of 0.156 × 0.117 × 0.5 mm³.

Data processing

The activation regions of the brain from bregma were selected using a brain maps atlas of rat [23]. And then, the regions of interest (ROI) were automatically defined by a paravision software (Bruker BioSpin, Ettlingen, Germany). An ROI manager analysis tool was used for the value of the signal intensity of the image (Image J, <https://imagej.nih.gov>), and the dispersion of the signal intensity of the ROI was analyzed using the interactive 3D surface plot v2.32 (spectrum LUT, grid size 128–512, lighting 0.27–0.8, max. 100%, min. 0%, Image J, <https://imagej.nih.gov>).

Statistical analysis

All the results were presented as mean ± SD. The mean signal intensity values of each ROI activated at different intensities in the two groups were compared (SNL and

sham group; SNL and GBP-treated SNL groups) using an independence *t*-test or one-way ANOVA. A *p*-value less than 0.05 ($P < 0.05$) was considered as a significant result. All statistical analyses were carried out using a Sigma stat (ver. 3.5, Systat Software Inc., Chicago, IL, USA).

Results

Confirmation of neuropathic pain induction in rats by SNL

Mechanical paw-withdrawal threshold was significantly decreased in the SNL rats as compared to the sham from the postoperative day (POD) 7. The attenuated threshold peaked on POD 14 (Fig. 1A). In order to investigate changes in the withdrawal threshold, GBP was treated at POD 14. Thirty min after GBP treatment, the withdrawal threshold began to recover and maintained for 90 min (Fig. 1A). Since the lowest threshold of the mechanical allodynia showed at POD 14, the thermal hyperalgesia test was performed only at that time. And, abnormal temperature sensing was also found in the SNL rats. The behavior response to cold with the acetone drop and paw-withdrawal latency to IR heat was decreased in the SNL rats (Fig. 1B). Sensing thresholds were recovered 90 min after GBP treatment to levels that were not statistically significant with the sham group (Fig. 1B).

Difference signal patterns of ROI between the SNL rats and sham rats

The patterns of signal enhancement were compared at the identical atlas level [23] in order to compare the activation regions of the rat brain following induction of neuropathic pain. Enhanced signal intensity was found in -8.30, -6.06, and -3.90 mm from the bregma (Fig. 2A). Among the selected ROI, 4 parts with a large difference in the signal intensity were found in the SNL rats. The signal intensity of the region 1, 2, 5, and 6 significantly increased in the SNL rats as compared to the sham rats (Fig. 2B). The areas corresponding to the signal increase are; [Region 1] RSPd: retrosplenial area, dorsal part; [Region 2] SC: superior colliculus; [Region 5] MO: motor area; [Region 6] SSp: primary somatosensory area.

GBP-induced attenuation patterns of the signal intensity of ROI

In order to investigate the functional deactivation re-

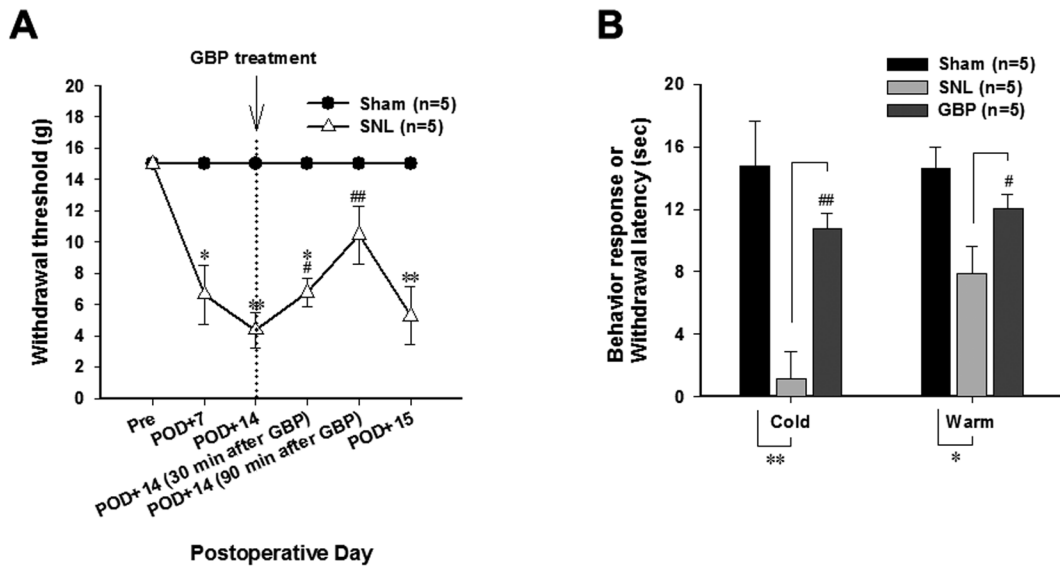


Fig. 1. Measurement of withdrawal threshold in the mechanical allodynia and the thermal hyperalgesia. (A) Comparison of Mechanical sensitivity, force (g) required for 50% threshold for paw withdrawal. (B) Cold sensitivity, paw-withdrawal duration to acetone, as a function of time. Plantar test for thermal sensitivity, paw-withdrawal latencies, performed at Infra Red (IR) intensities, * $P < 0.05$ and ** $P < 0.001$ as compared to the sham (t -test); # $P < 0.05$ and ## $P < 0.001$ as compared to the Sham and POD+14 SNL (t -test and one-way ANOVA). Results are mean \pm SD.

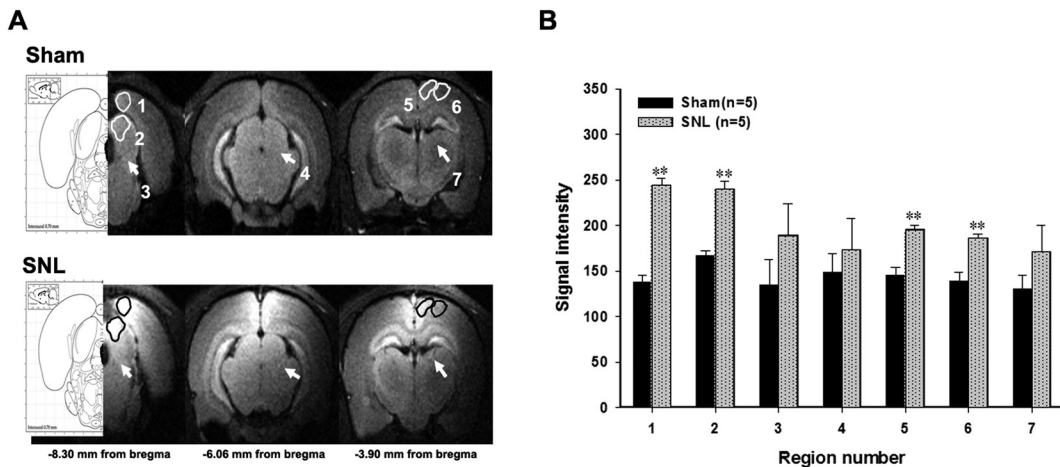


Fig. 2. 2D T1-weighted spin-echo MEMRI images. (A) The different signal enhancements of the two groups at the identical atlas level were compared [23]. The atlas levels are 46 (AP, -8.30 mm from bregma), 39 (AP, -6.06 mm from bregma), and 32 (AP, -3.90 mm) [23]. (B) Quantitative analysis of the signal intensity between the sham and the SNL rats. ** $P < 0.001$ compared to the sham (t -test). Results are mean \pm SD.

regions of the brain, changes in the signal intensity were analyzed two times at 30 and 90 min after GBP treatment (Fig. 3A). The signal intensity was decreased in the area -8.30 , -6.06 and -3.90 mm from the bregma (Fig. 3B). The dispersion of the signal intensity was indicated using a 3D surface plot. The signal intensity was evenly decreased in the selected areas (region 1–6) as time went

on. It was decreased to the minimum 28.5% and to the maximum 47.9% as a result of signal ratio between the SNL rats and the GBP-administered SNL rats (Fig. 3C). In the quantitative analysis, the signal intensity of the Region 1 was 251.7 ± 14.4 before GBP administration, and it began to decrease significantly 30 min after the GBP administration. According to the time intervals,

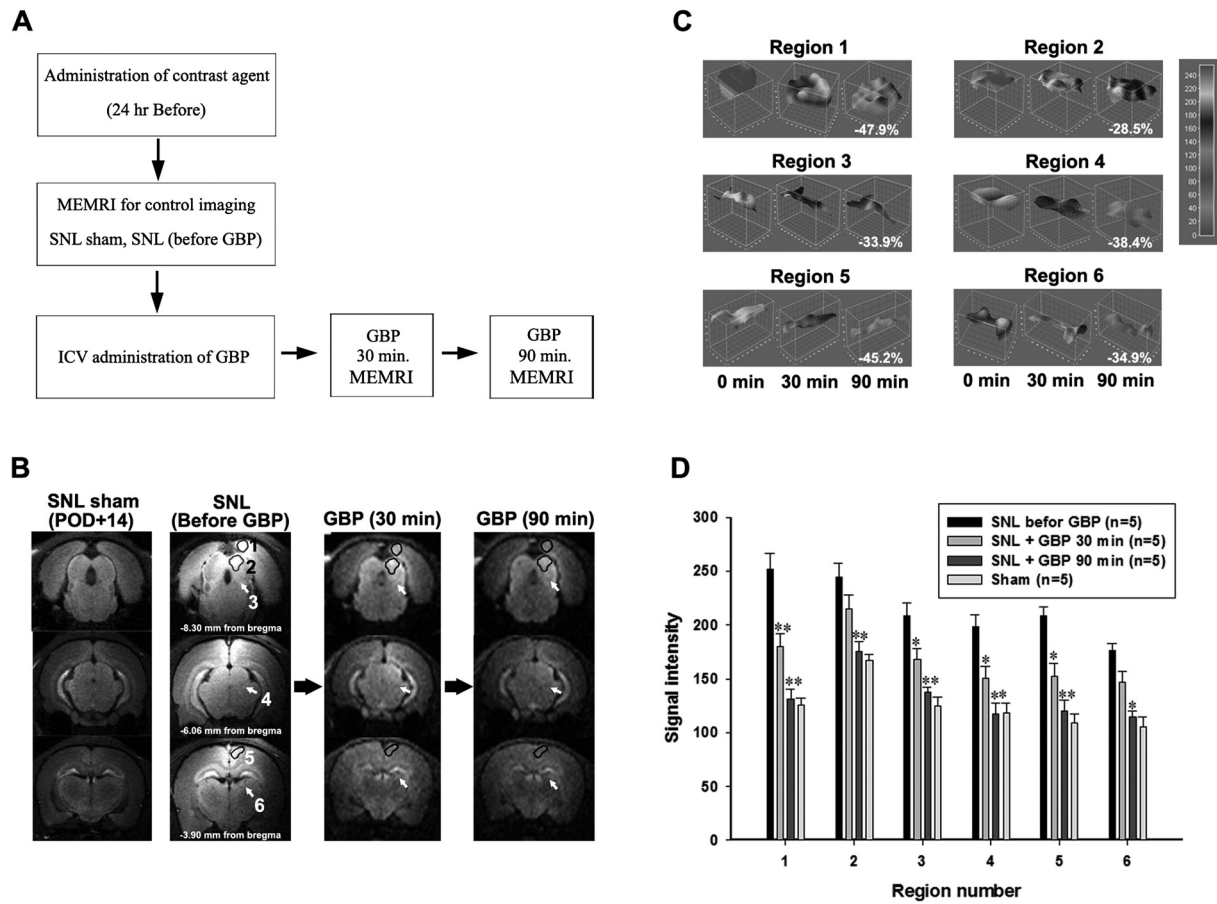


Fig. 3. Observation of the signal intensity via MEMRI following GBP administration. (A) Strategy for MEMRI with GBP administration. (B) Phased attenuation of the signal intensity in the brain due to GBP administration (C) Phased change pattern analysis of the signal intensity of ROI. (D) Quantitative analysis of the signal intensity following GBP administration. * $P < 0.05$ and ** $P < 0.001$ as compared to the SNL (before GBP) (one-way ANOVA). Results are mean \pm SD. [Region 1] RSPd: retrosplenial area, dorsal part; [Region 2] SC: superior colliculus; [Region 3] IC: inferior colliculus; [Region 4] PAG: periaqueductal gray; [Region 5] MO: motor area; [Region 6] LH: lateral habenula, CL: central lateral nucleus thalamus, LP: lateral posterior nucleus thalamus.

signal intensities were 180.2 ± 11 at 30 min and 131.3 ± 8.9 at 90 min. The signal intensity of Region 1 of the sham rat was 125.3 ± 7 (Fig. 3D). The signal intensities of other regions were 244.4 ± 12 (Region 2), 208.6 ± 11 (Region 3), 198.4 ± 10 (Region 4), 208.7 ± 7 (Region 5), 176.1 ± 7 (Region 6) before GBP administration. It was also begun to decrease at 30 min after the GBP administration (Region 2: 215.1 ± 12 ; Region 3: 167.4 ± 11 ; Region 4: 150.9 ± 10 ; Region 5: 152.5 ± 12 ; Region 6: 146.8 ± 10). And the signal intensity of all regions was significantly decreased (Region 2: 174.8 ± 9 ; Region 3: 137.4 ± 4 ; Region 4: 117.7 ± 10 ; Region 5: 120.0 ± 9 ; Region 6: 114.8 ± 5) as the sham group (Region 2: 167.2 ± 5 ; Region 3: 124.4 ± 8 ; Region 4: 118.2 ± 9 ; Region 5: 109.2 ± 8 ; Region 6: 105.1 ± 9) at 90 min. The

signal intensity of the Region 2 and 6 was decreased at 90 min only (Fig. 3D).

Discussion

In this study, neuropathic pain-induced brain functional activity was investigated using an animal MEMRI system. The functional activity in the rat brain regions were increased by SNL, and the activity was chronologically decreased after the administration of GBP. From these results, it is possible to find the regions of the brain related with neuropathic pain.

MEMRI method was used to reveal anatomical structures for the analysis of brain activity [24]. And, many studies have explored the side effect of Mn^{2+} by toxic-

ity [20, 22]. A major problem of high levels of Mn^{2+} is to cause movement disorders [20]. Therefore, we titrated the non-toxic and optimal concentration of the agent while monitoring the physiological status of the animals [13]. We have found that 20 mM of $MnCl_2$ in a volume of 50 μ l was a physiologically stable dose for intracerebroventricular (ICV) administration, and it provided an optimal image for the structural analysis of a rat brain at 24 h after administration [13]. Therefore, we conducted the study in accordance with these conditions.

According to the signal analysis of the SNL rats, the increased signal was found in the posterior association area of parietal region, superior colliculus, inferior colliculus, primary somatosensory cortex (SSp), retrosplenial area, and the cingulum bundle. The cerebral cortex is divided into four major lobes: frontal, parietal, occipital, and temporal. The central sulcus divides the frontal and parietal lobes and is the key landmark for locating the primary motor and somatosensory cortex. It processes this afferent information resulting from the detection of the mechanical stimuli. The parietal lobe plays important roles in integrating sensory information from various parts of the body. The inferior colliculus is the principal midbrain nucleus of the auditory pathway and receives input from several more peripheral brainstem nuclei [10, 27].

Therefore, recent studies have shown that a mesencephalic reticular formation is involved in pain perception, and that many spinal and trigeminal nociceptive neurons project to structures in the midbrain, especially the PAG, inferior colliculus, cuneiform nuclei. The retrosplenial area is part of the cingulate cortex and considered part of the limbic lobe. The cingulum bundle contains fibers that project from the anterior thalamic nuclei to the anterior cingulate cortex. Using evoked potentials, Foltz and White [9] demonstrated that the cingulum bundle connects the medial frontal cortex, anterior thalamic nuclei, and the rostral midline and intralaminar nuclei. The cingulum bundle is part of a widespread limbic circuit that includes the fornix, mammillary bodies, anterior thalamic nuclei and cingulate cortex [26]. In other words, the cingulum bundle, a major pathway of the limbic system, is a structure which is involved in the cortical emotion control. That is, the cingulum bundle includes the fiber that links the information received from the thalamus to the cingulate cortex.

GBP-mediated inhibition of voltage-gated Ca^{2+} channels results in a reduction of excitatory transmission in

the spinal cord dorsal horn, consistent with an inhibition of spinal transmission [21]. Alpha2delta subunit has been documented as its main target and its specific binding to this subunit is described to produce different actions responsible for pain attenuation [4].

In this study, the neuropathic pain-evoked rats showed strong signal intensity in the brain. We therefore hypothesized that if the results of these images are increased signal intensity, due to pain perception, the signal intensity should be attenuated by GBP administered. And, the present study applied GBP to confirm the attenuation patterns of signal intensity. As a result of consecutive scans, each group showed the attenuation patterns of the signal intensity. It was found that the analgesic effect of GBP administered into CSF works extensively in the entire area of the brain; it starts working at 30 min after the drug administration, with maximum effects at 90 min. Our findings are consistent with previous studies, and it demonstrates the typical characteristics of GBP related analgesic effect [14, 21].

In the functional activation study of the brain using MEMRI, the signal intensities of numerous brain parts of the SNL rats clearly differed from those of the sham rats. GBP administration led to the attenuation of cerebral signal intensity. By considering the findings together, SNL induced-neuropathic pain is transmitted to the thalamus through the lateral spinothalamic tract, and later on the impulse is transmitted to the cingulum bundle and part of the limbic system, thereby reacting to pain stimulation in the SSp and parietal region. These studies will be help in further researches such as analgesic effect on neuropathic pain to specific target those brain regions.

Conflict of Interest

Author Keun-Yeong Jeong declares that he has no conflict of interest. Author Ji-Hyuk Kang declares that he has no conflict of interest.

References

1. Baik, E., Chung, J.M., and Chung, K. 2003. Peripheral norepinephrine exacerbates neuritis-induced hyperalgesia. *J. Pain* 4: 212–221. [Medline] [CrossRef]
2. Barad, M.J., Ueno, T., Younger, J., Chatterjee, N., and Mackey, S. 2014. Complex regional pain syndrome is associated with structural abnormalities in pain-related regions of the human brain. *J. Pain* 15: 197–203. [Medline] [CrossRef]

3. Chaplan, S.R., Bach, F.W., Pogrel, J.W., Chung, J.M., and Yaksh, T.L. 1994. Quantitative assessment of tactile allodynia in the rat paw. *J. Neurosci. Methods* 53: 55–63. [[Medline](#)] [[CrossRef](#)]
4. Cheng, J.K. and Chiou, L.C. 2006. Mechanisms of the antinociceptive action of gabapentin. *J. Pharmacol. Sci.* 100: 471–486. [[Medline](#)] [[CrossRef](#)]
5. Chung, J.M., Kim, H.K., and Chung, K. 2004. Segmental spinal nerve ligation model of neuropathic pain. *Methods Mol. Med.* 99: 35–45. [[Medline](#)]
6. Decosterd, I. and Woolf, C.J. 2000. Spared nerve injury: an animal model of persistent peripheral neuropathic pain. *Pain* 87: 149–158. [[Medline](#)] [[CrossRef](#)]
7. Eck, J., Richter, M., Straube, T., Miltner, W.H., and Weiss, T. 2011. Affective brain regions are activated during the processing of pain-related words in migraine patients. *Pain* 152: 1104–1113. [[Medline](#)] [[CrossRef](#)]
8. Eschenko, O., Canals, S., Simanova, I., Beyerlein, M., Murayama, Y., and Logothetis, N.K. 2010. Mapping of functional brain activity in freely behaving rats during voluntary running using manganese-enhanced MRI: implication for longitudinal studies. *Neuroimage* 49: 2544–2555. [[Medline](#)] [[CrossRef](#)]
9. Foltz, E.L. and White, L.E. Jr. 1962. Pain “relief” by frontal cingulumotomy. *J. Neurosurg.* 19: 89–100. [[Medline](#)] [[CrossRef](#)]
10. Harris, J.A. 1998. Using c-fos as a neural marker of pain. *Brain Res. Bull.* 45: 1–8. [[Medline](#)] [[CrossRef](#)]
11. Jackels, S.C., Kroos, B.R., Hinson, W.H., Karstaedt, N., and Moran, P.R. 1986. Paramagnetic macrocyclic complexes as contrast agents for MR imaging: proton nuclear relaxation rate enhancement in aqueous solution and in rat tissues. *Radiology* 159: 525–530. [[Medline](#)] [[CrossRef](#)]
12. Jensen, T.S., Baron, R., Haanpää, M., Kalso, E., Loeser, J.D., Rice, A.S., and Treede, R.D. 2011. A new definition of neuropathic pain. *Pain* 152: 2204–2205. [[Medline](#)] [[CrossRef](#)]
13. Jeong, K.Y., Lee, C., Cho, J.H., Kang, J.H., and Na, H.S. 2012. New method of manganese-enhanced Magnetic Resonance Imaging (MEMRI) for rat brain research. *Exp. Anim.* 61: 157–164. [[Medline](#)] [[CrossRef](#)]
14. Kazi, J.A. and Abu-Hassan, M.I. 2011. Gabapentin completely attenuated the acute morphine-induced c-Fos expression in the rat nucleus accumbens. *J. Mol. Neurosci.* 45: 101–109. [[Medline](#)] [[CrossRef](#)]
15. Koltzenburg, M. and Scadding, J.W. Neuropathic pain: bench to bedside. London: The Royal Society of Medicine Press; 2005.
16. Lee, B.H., Won, R., Baik, E.J., Lee, S.H., and Moon, C.H. 2000. An animal model of neuropathic pain employing injury to the sciatic nerve branches. *Neuroreport* 11: 657–661. [[Medline](#)] [[CrossRef](#)]
17. Manning, J.P., Richards, D.A., and Bowery, N.G. 2003. Pharmacology of absence epilepsy. *Trends Pharmacol. Sci.* 24: 542–549. [[Medline](#)] [[CrossRef](#)]
18. Na, H.S., Choi, S., Kim, J., Park, J., and Shin, H.S. 2008. Attenuated neuropathic pain in Cav3.1 null mice. *Mol. Cells* 25: 242–246. [[Medline](#)]
19. Ogawa, S., Lee, T.M., Kay, A.R., and Tank, D.W. 1990. Brain magnetic resonance imaging with contrast dependent on blood oxygenation. *Proc. Natl. Acad. Sci. USA* 87: 9868–9872. [[Medline](#)] [[CrossRef](#)]
20. Pautler, R.G. 2006. Biological applications of manganese-enhanced magnetic resonance imaging. *Methods Mol. Med.* 124: 365–386. [[Medline](#)]
21. Shimoyama, M., Shimoyama, N., and Hori, Y. 2000. Gabapentin affects glutamatergic excitatory neurotransmission in the rat dorsal horn. *Pain* 85: 405–414. [[Medline](#)] [[CrossRef](#)]
22. Silva, A.C., Lee, J.H., Aoki, I., and Koretsky, A.P. 2004. Manganese-enhanced magnetic resonance imaging (MEMRI): methodological and practical considerations. *NMR Biomed.* 17: 532–543. [[Medline](#)] [[CrossRef](#)]
23. Swanson, L.W. Brain maps III: structure of the rat brain. Amsterdam; London: Elsevier Academic Press; 2004.
24. Takeda, A., Kodama, Y., Ishiwatari, S., and Okada, S. 1998. Manganese transport in the neural circuit of rat CNS. *Brain Res. Bull.* 45: 149–152. [[Medline](#)] [[CrossRef](#)]
25. Taylor, C.P. 1997. Mechanisms of action of gabapentin. *Rev. Neurol. (Paris)* 153:(Suppl 1): S39–S45. [[Medline](#)]
26. Vaccarino, A.L. and Melzack, R. 1992. Temporal processes of formalin pain: differential role of the cingulum bundle, fornix pathway and medial bulboreticular formation. *Pain* 49: 257–271. [[Medline](#)] [[CrossRef](#)]
27. Zambreau, L., Wise, R.G., Brooks, J.C., Iannetti, G.D., and Tracey, I. 2005. A role for the brainstem in central sensitization in humans. Evidence from functional magnetic resonance imaging. *Pain* 114: 397–407. [[Medline](#)] [[CrossRef](#)]